TIME AND FREQUENCY COMPARISONS BETWEEN FOUR EUROPEAN TIMING INSTITUTES AND NIST USING MULTIPLE TECHNIQUES

A. Bauch[(1)], J. Achkar[(2)], R. Dach[(3)], R. Hlavac[(4)], L. Lorini[(5)], T. Parker[(6)], G. Petit[(7)], and P. Uhrich[(2)]
(1) Physikalisch-Technische Bundesanstalt Braunschweig, Germany
(2) Laboratoire National de Métrologie et d'Essais – Observatoire de Paris / Systèmes de Référence Temps Espace, Paris, France
(3) Astronomical Institute, University of Bern, Switzerland
(4) National Physical Laboratory, Teddington, UK
(5) Istituto Elettrotecnico Nazionale Galileo Ferraris, Torino, Italy
(6) National Institute of Standards and Technology, Boulder, Colorado, USA
(7) Bureau International des Poids et Mesures, Sèvres, France
Corresponding Author: A. Bauch, PTB, Bundesallee 100, 38116 Braunschweig, Germany, e-mail: andreas.bauch@ptb.de

ABSTRACT

Istituto Elettrotecnico Nazionale Galileo Ferraris (IEN), National Institute of Standards and Technology (NIST), National Physical Laboratory (NPL), Laboratoire National de Métrologie et d'Essais – Observatoire de Paris / Systèmes de Référence Temps Espace (OP), and Physikalisch-Technische Bundesanstalt (PTB) performed an intense comparison campaign of selected frequency references maintained in their laboratories during about 25 days in October/November 2004. The active hydrogen maser reference standards used at all laboratories served at the same time as frequency references for the institutes' fountain frequency standards. The fountains of IEN, NPL, and OP were operated for most of the time during the same period, and results of the fountain comparisons are given in an accompanying paper. Three techniques of frequency (and time) comparisons were employed. Going beyond the standard procedures, two-way satellite time and frequency transfer was performed in an intensified measurement schedule of 12 equally spaced measurements per day. The data of dual frequency geodetic GPS receivers were processed to yield an ionosphere-free linear combination of the code observations from both GPS frequencies, typically referred to as TAI P3 analysis. Last but not least, the same GPS raw data were separately processed allowing GPS carrier-phase based frequency comparisons to be made. These showed the lowest instability at short averaging times of all of the methods. The instability was at the level of 1 part in 10^{15} at one-day averaging time, similar to what was achieved with TWSTFT. The GPS TAI P3 analysis is capable of giving a similar quality of data provided that averaging over two days or longer is acceptable. The analysis presented here shows that all techniques provide the same mean frequency difference between the standards involved within the measurement uncertainty of a few parts in 10^{16}.

1. INTRODUCTION

The study of time and frequency transfer is an important sector of time and frequency metrology in general since it is essential for the wide application of state-of-the-art frequency standards. In recent years, research into primary frequency standards has led to several devices whose uncertainty to realize the SI second is at the level of one part in 10^{15} or below and whose frequency instability is good enough to verify this accuracy during averaging times of one day or even below [1-5]. Data from these clocks have been regularly used by the Bureau International des Poids et Mesures (BIPM) as an input for the realization of International Atomic Time (TAI) and of Coordinated Universal Time (UTC). Generally speaking, two different methods of time transfer have traditionally been used by BIPM for maintaining the network of participating laboratories, Global Positioning System (GPS) common view (CV) and two-way satellite time and frequency transfer (TWSTFT) via geostationary satellites [6, 7]. Classical GPS C/A code analysis is not discussed in this article since it does not provide the required measurement resolution. A step forward has been the use of geodetic GPS receivers providing dual frequency code observables which allow the so-called TAI P3 analysis to be made [8]. The use of GPS phase observables for frequency transfer has been proposed for similar purposes [9, 10] and has already been used to compare the fountain clocks CSF1 of the Physikalisch-Technische Bundesanstalt, Germany (PTB), and F1 of the National Institute of Standards and Technology, USA (NIST) [11].

Three further institutes, the UK National Physical Laboratory (NPL), the Italian Istituto Elettrotecnico Nazionale Galileo Ferraris (IEN), and the French Laboratoire National de Métrologie et d'Essais – Observatoire de Paris / Systèmes de Référence Temps Espace (abbreviated as OP throughout the paper), agreed with NIST and PTB on a campaign of comparisons among their fountain type primary frequency standards, to be effected during 20 to 25

Tab.1 Institutes involved and equipment in use

Institute	Clock or frequency reference	TWSTFT modem	IGS station code	GPS receiver antenna
IEN	HM: Symmetricom, UTC(IEN): Agilent 5071	MITREX	IENG	ASHTECH Z-XII3T, ASH701945C_M
NPL	HM: Symmetricom, representing UTC(NPL)	SATRE	NPLD	ASHTECH Z-XII3T, AOAD/M_T
NIST	HM: Symmetricom, representing UTC(NIST)	SATRE	NISU	NOV EURO4-1.00-222, NOV600
OP	HM: Symmetricom	SATRE	OPMT	ASHTECH Z-XII3T, 3S-02-TSADM
PTB	HM: VREMYA-CH UTC(PTB): primary clock CS2	SATRE	PTBB	ASHTECH Z-XII3T, ASH700936E

Tab. 2 TWSTFT measurement schedule and Mitrex codes assigned to the stations. The receive (RX)and transmit (TX) frequency in Europe differs for the inner-European and the US-Europe link.

Measurements during each second hour of a day in UTC First	Last	Duration	OP		NPL		PTB		IEN		NIST	
hh:mm:ss	Hh:mm:ss	(s)	TX	RX	TX	RX	TX	RX	TX	RX	TX	RX
00:10:00	00:11:59	120	0	1	1	0						
00:13:00	00:14:59	120					4	6	6	4		
00:19:00	00:20:59	120	0	4			4	0				
00:22:00	00:23:59	120			1	4	4	1				
00:25:00	00:26:59	120	0	6					6	0		
00:28:00	00:29:59	120			1	6			6	1		
00:37:00	00:38:59	120	0	6							6	0
00:40:00	00:41:59	120			1	6					6	1
00:49:00	00:50:29	120					4	6			6	4
00:52:00	00:53:59	120							6	6	6	6

days in October and November 2004, Modified Julian Days (MJD) between 53304 and 53329. The five institutes are part of a regularly operated TWSTFT network, and for the duration of the campaign an intensified measurement schedule was agreed upon. The institutes also operate geodetic GPS receivers and their stations belong to the network of sites of the International GPS Service (IGS) [12]. The institutes obtained the support of the Astronomical Institute of the University of Bern (AIUB), Switzerland, which processes the GPS data with an innovative software, providing long-term monotonous series of clock solutions for the stations involved with extremely high resolution, based entirely on the GPS carrier phase (GPS CP) [13]. Last but not least, the BIPM provided the TAI P3 analysis of the GPS data [8].

It finally turned out that the fountains of NIST and PTB were not ready to provide data during the campaign, so that fountain comparisons were only carried out between the IEN CsF1, the NPL CsF1, and the OP-FO2. The results are reported in a separate paper [14]. Also in this paper, particular attention is given to the properties of the time links between the three relevant institutes. But the analysis included all available links and techniques, which has not been done before in such depth. Clearly, only a selection of the results could be presented in this paper, and we aimed at showing the achievable performance as well as pointing to some features that were not understood. Results beyond those presented here will be made available elsewhere.

In the following sections we will detail the equipment and time transfer techniques involved before presenting results for each technique and for inter-comparisons among techniques.

2. DESCRIPTION OF HARDWARE AND TIME TRANSFER TECHNIQUES

2.1 Station equipment

In Tab. 1, we describe the equipment involved in the participating stations. In all cases, the hydrogen masers served as the fly-wheel oscillators for comparisons with the fountain frequency standards, and the maser signals were connected to the time transfer equipment. This most straightforward configuration is depicted in Fig. 1, indicating the three different time transfer techniques connecting the masers at the remote sites. In the cases of NIST and NPL, the maser output represented the local UTC scale, UTC(NIST) [15], and UTC(NPL), respectively. In the case of IEN and PTB, however, the GPS receiver was connected to UTC(IEN) and UTC(PTB), respectively, which are derived from caesium clocks, a

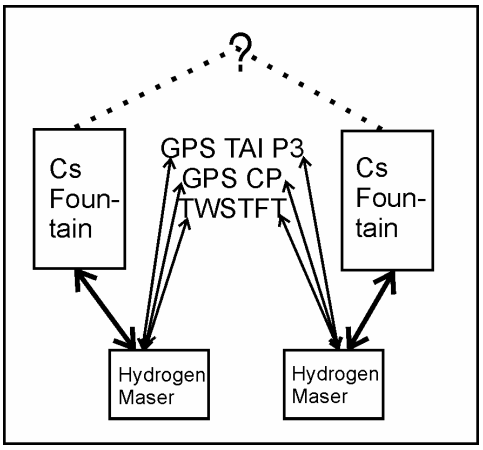

Fig. 1 Configuration of frequency comparisons during the campaign, the frequency standards at left and at right, respectively, are operated in different institutes.

commercial model at IEN, and the primary clock CS2 at PTB [16]. As a result, further steps in the data analysis were required to reference all techniques to the same frequency standard. The time differences UTC(PTB) – HM(PTB) were available only on an hourly basis and this dictated the minimum averaging time for GPS CP and GPS TAI P3 data presented below. At IEN the corresponding measurements were taken more frequently so that a more complete data analysis could have been performed in principle. This has, however, not been included in this paper.
In the sections dealing with results links are often only denoted by the station acronyms, e. g. by PTB-NPL for simplicity. In the graphs, connecting lines serve the purpose to guide the eye.

2.2 TWSTFT analysis

The stations involved performed TWSTFT, co-ordinated by the CCTF Working Group on TWSTFT, following standard procedures: At each pair of stations, named A and B for now, a characteristic pseudo-random noise (PRN) spread spectrum signal which is designated by a certain Mitrex code (see Tab. 2), synchronous with the local 1 PPS time references $T(\mathrm{Ref_A})$ and $T(\mathrm{Ref_B})$, respectively, is generated on a 70 MHz intermediate frequency. It is up-converted to the rf region (Ku-band, up link at about 14 GHz) and transmitted to a geostationary telecommunication satellite, in the present case the IS-903 of Intelsat Corp., located at 325.5° East. At the satellite, the signal is translated to the downlink frequency (about 12 GHz) and sent back to earth. The time of arrival (TOA) of the PRN coded signal from station A (B) is determined at station B (A) by cross-correlation of the received and down-converted PRN signal with a local replica of the same PRN code, synchronous with the local reference clock. TOA measurements are made each second during sessions of two minutes per station pair. The time differences exhibited a 1 σ - standard deviation of below 400 ps in favourable cases, but going up to almost 1.5 ns for some links. This fact is discussed further below. At the end of a session, a quadratic function is fitted to the data and the TOA midpoint values derived from the fit are exchanged via file transfer through the internet. This allows the quantity of interest, $T(\mathrm{Ref_A}) - T(\mathrm{Ref_B})$, to be calculated, as explained by Kirchner [7] and in an ITU-R Recommendation [17]. For the purpose of an intense comparison, TWSTFT sessions were performed nominally once every two hours. The data sets contained very few gaps, on some links about 315 out of 320 possible data points were recorded, while in a few cases about 20 data points were missing. The TWSTFT measurement schedule including the assigned Mitrex codes is reproduced in Tab. 2. One can recognize that measurements were not taken perfectly simultaneously.

2.3 GPS carrier- phase analysis

All five participating institutes contribute to the IGS network. The observations are provided in RINEX format and contain pseudorange (code) and carrier-phase measurements from the two GPS frequencies for all tracked satellites with a sampling interval of 30 seconds. The midnight epoch is missing in the observation files from the stations OPMT and NPLD, but the receiver tracked continuously. Therefore, this has no effect on the GPS CP solution (apart from the missing results for this particular epoch).
The GPS CP analysis was performed at AIUB using the Bernese GPS Software, Version 5.1 [18]. The solutions are based on the contributions to the IGS of the Analysis Center CODE (Center for Orbit Determination in Europe) hosted at AIUB. CODE is a collaboration between the Astronomical Institute of the University of Bern (AIUB), the Federal Office of Topography (Swisstopo, Switzerland), the Federal Agency for Cartography and Geodesy (BKG, Germany), and the Institut Géographique National (IGN, France). The satellite orbits, Earth orientation parameters, station coordinates, and troposphere delays are introduced from the (geodetic) three-day, double-difference solution calculated for the IGS at CODE. In the clock estimation procedure the receiver and satellite clocks are solved for along with other parameters (e.g. phase ambiguities). The result is a network solution with a set of consistent receiver and satellite clock corrections for each epoch. All receiver clock comparisons (baselines) are extracted from this network solution, hence all loops of extracted baselines give zero. The GPS CP method imposes no a priori information on the clocks by any filtering. The clock corrections are freely estimated for each epoch. The GPS CP solution used in the current campaign contains no day boundary discontinuities because the phase ambiguities from the daily data processing are reconnected before estimating the clock parameters. As in addition frequency transfer has been the main interest, the code observations have been discarded.

Such an approach, using only phase information and neglecting code information, has never been made before for a several-weeks long campaign by the AIUB and, as far as we know, has also not been published by any other group. A detailed discussion is given in [13].

2.4 GPS TAI P3 analysis

The GPS TAI P3 technique has been used since 2002 by the BIPM, with about 15 participating laboratories equipped with geodetic GPS receivers. The dual-frequency P1 and P2 observables delivered by the receivers are linearly combined to form the ionosphere-free P3 observable. They are transferred to the CGGTTS format used in standard GPS time transfer [8, 19] using locally recorded broadcast GPS parameters. This format dictates in particular the sampling rhythm for the time differences of 16 minutes, and that the tracking schedule shifts in time from day to day. The CGGTTS data files are gathered by BIPM and used to compute time links after applying different corrections: precise satellite orbits and clocks obtained from the IGS, and station displacement due to solid Earth tides. The six time links (no data from NIST were processed) were computed using the common-view technique. For each 16-minute interval, all available common-view differences were formed and averaged with a weighting scheme based on the satellite elevation, after a first screening for big outliers. BIPM provided unsmoothed and Vondrak smoothed data, the results shown below were derived from the former.

3. RESULTS

3.1 General observations

To give an example, data obtained on the link NPL – OP during one day are depicted in Fig. 2. With a small offset in the epoch of data taking, the TWSTFT measurements once every two hours (red dots, one data point missing) follow the GPS CP data (open blue circles) obtained at the full hour. As it is important to eliminate as far as possible the effect of clock instabilities when comparing the two techniques (see Section 4.1), in such cases the GPS CP measurement taken closest in time to the TWSTFT measurement (see Tab. 2) was used. The TAI P3 data at 16-minute intervals (black dots) are offset by 2 ns for clarity.

A few data points were in general missing for all links, and even complete GPS TAI P3 data would not represent a continuos time series. In all stability plots, however, the minimum τ was chosen as the nominal value irrespective of the actual mean separation in time between measurements as the availability was quite high and the impact of missing data on the plots was considered as minor in the current study.

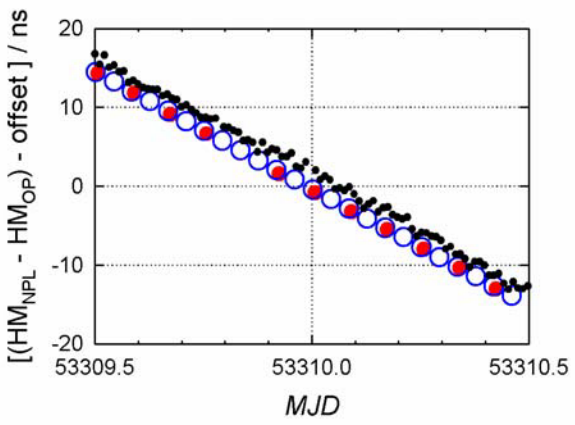

Fig. 2 Example of data collected during one day on the NPL – OP link; GPS CP (open circles), TWSTFT (red dots), and GPS TAI P3 (black dots), offset by 2 ns for clarity.

In Fig. 3 the general performance of the hydrogen masers involved is illustrated. Here UTC(NIST) was chosen as the common reference, and GPS CP time differences to all other masers at an hourly separation were evaluated, linear trends were subtracted, and the residuals to the linear fitted functions were plotted. It can be ssen that the NPL maser performed very well except for a kink towards the end of the campaign, and the OP maser had a significant non-linear frequency change during the period.

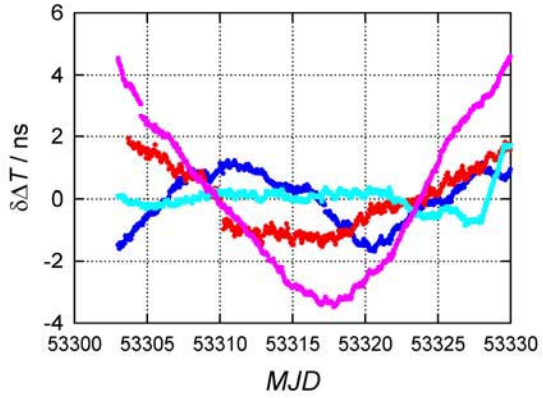

Fig. 3 General characteristics of the frequency standards at NIST (common reference), IEN (red), NPL (cyan), OP (magenta), and PTB (blue) during the study period, MJD 53303 – 53330; residuals to linear fits to time differences UTC(NIST) – local references obtained via GPS CP.

3.2 TWSTFT results

The extended TWSTFT schedule provided valuable insight in the stability of TWSTFT links. At an averaging time of about one day the measurement noise (white phase noise) tends to become insignificant compared to the instability of the masers involved. It turned out that links to NIST, which utilize a different transponder on the satellite than the intra-European links, are in all cases more noisy. Fig. 4 showing PTB-NPL and PTB-NIST data may serve as an illustration, and Fig. 6 below gives further proof.

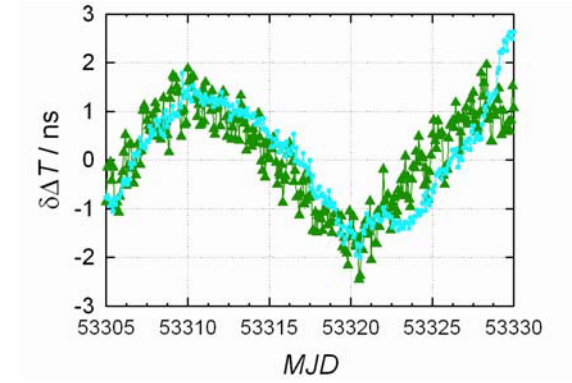

Fig. 4 Time differences PTB – NPL (cyan), and PTB – NIST (green) obtained via TWSTFT, mean time offset and mean rate removed.

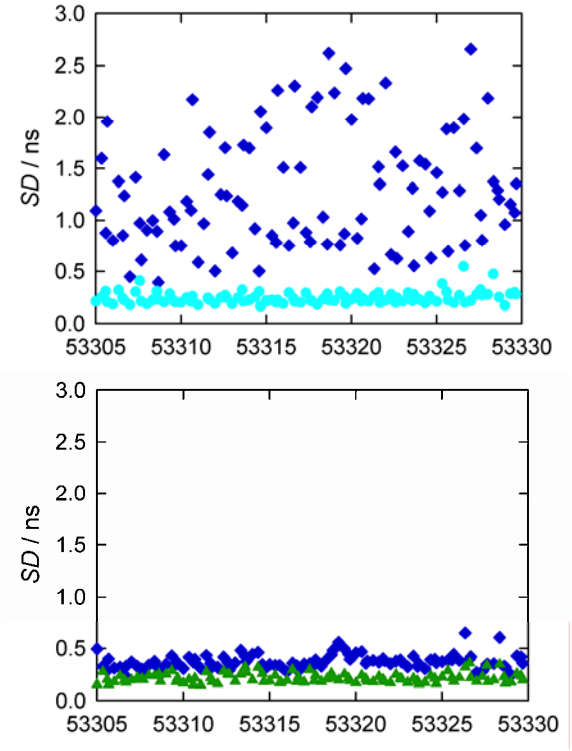

Fig. 5 Observed instability of the TWSTFT data for the links PTB-NPL (upper) and PTB-NIST (lower); standard deviation in ns of the individual one second measurement data recorded at PTB (blue diamonds), NPL (cyan circles) and NIST (green triangles), respectively, around the quadratic regression function during the comparison campaign.

Here we find $\sigma_X(\tau = 2\ \text{h}, \text{PTB-NPL}) = 0.12$ ns, and $\sigma_X(\tau = 2\ \text{h}, \text{PTB-NIST}) = 0.28$ ns. These findings are seemingly in contradiction to the observed standard deviation of individual one second measurement results around the quadratic regression function obtained at the respective sites which are reported in Fig. 5. Apparently, the short-term measurement noise whose origin is not yet understood is efficiently averaged, and longer term variations dominate the links to the US. Presumably, these are in general due to the longer baseline which may have an impact due to unaccounted satellite motion (respectively incorrect time tagging of the measurements) or due to uncorrelated environmental effects. Errors due to unaccounted satellite motion are distinctively sinusoidal in shape (with a one day period), and this was not observed. The temperature sensitivity of the NIST ground station as well as the unaccounted ionospheric delay (small at Ku-band anyway) can be ruled out as causes. What remains as a potential cause is the instability of the transponder on the satellite, which was also noted by the United States Naval Observatory (which is routinely part of the TWSTFT network, but which did not participate in the extended measurement schedule).

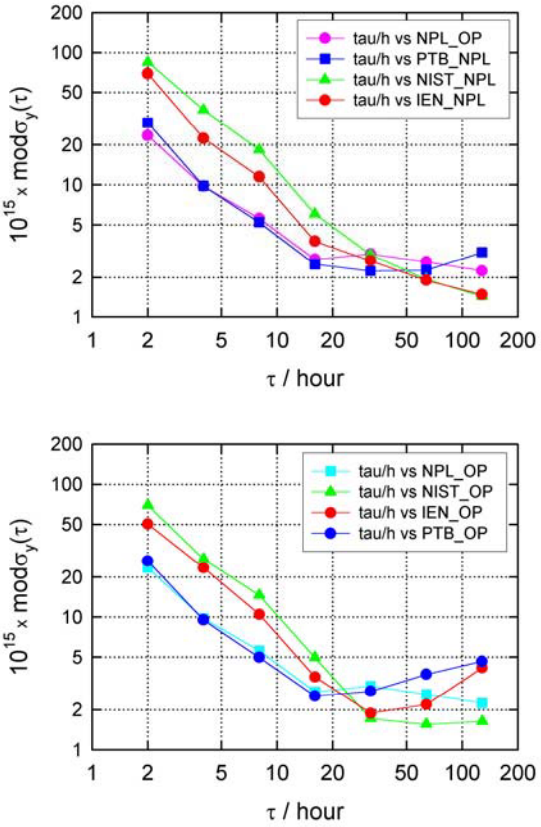

Fig. 6 Relative frequency instability, expressed by $\text{mod}\sigma_y(\tau)$, in the TWSTFT comparison of masers at NPL (upper graph) and OP (lower graph) to the other participating stations explained in the insets to the figures.

The frequency instability obtained from the TWSTFT comparisons of all institutes with respect to the masers at OP and NPL is depicted in Fig. 6. The lowest measurement noise is observed in the links between NPL, OP, and PTB. The slightly excessive noise in the links to IEN is probably due to the older TWSTFT modem (of Mitrex type) still used at IEN. When forming the so-called "closure" (OP – NPL) + (PTB – OP) + (NPL – PTB) a 0.34 ns deviation from zero is observed, which can be partially explained by the mean clock rate of the OP maser of about –28 ns/day and the fact that the two measurements involving OP

are separated by about 9 minutes (see Tab. 2). A real closure error would point to the fact that the signal delays in the receive path of at least one of the stations depend on the received PRN code. The closure data exhibited a standard deviation around the mean value of 0.14 ns, which represents the combined measurement noise of three TWSTFT measurements plus the time stability of the frequency standards over 9 minutes. The closure results are depicted in Fig. 7.

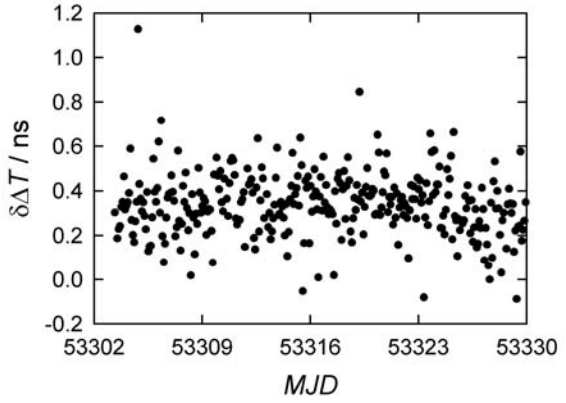

Fig. 7 TWSTFT "closure" results – in total 312 data points - combining the three individual measurements OP – NPL, PTB – OP, and NPL – PTB collected during the campaign according to the schedule represented in Tab. 2

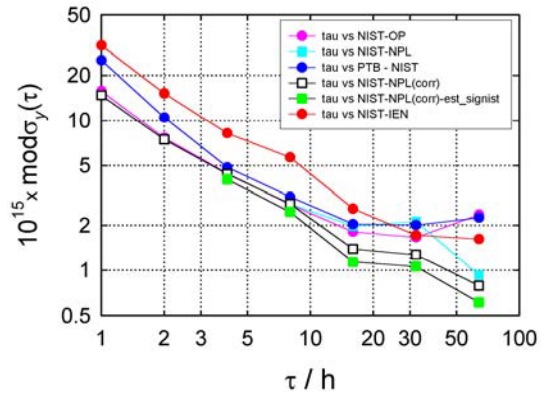

Fig. 8 Relative frequency instability, expressed by $\mathrm{mod}\sigma_y(\tau)$, in the GPS CP comparison of UTC(NIST) with masers at OP, NPL, PTB, and IEN, see coding of symbols in the inset. Additional plots: instability after removal of the frequency step of the NPL maser (open squares), and after subtracting thereof the estimated instability of UTC(NIST) (green squares).

3.3 GPS CP results

The GPS CP data analysis revealed a very low level of measurement noise and thus an assessment of the instability of the frequency standards involved at the shortest averaging time was possible. As explained before, the original data of AIUB had UTC(PTB) and UTC(IEN) as the references. In order to get a meaningful comparison of the three frequency transfer techniques, local measurements were used to provide the link to the masers at PTB and IEN, and only hourly data were dealt with. The results of GPS CP frequency comparisons were previously used as illustration (see Fig. 3). In Fig. 8 we provide the frequency instability derived from these data. Two plots were added which give further proof of the merits of this technique. When the frequency step of the NPL maser (see Fig. 2-3) after MJD 53328 is removed from the data, the NPL-NIST instability is further lowered (open squares). The frequency instability of UTC(NIST) has been estimated based on an analysis with respect to the group of active hydrogen masers in operation at NIST [15]. Subtracting this noise contribution from the previously mentioned data should allow the combined instability of the frequency transfer and the NPL maser (green squares) to be assessed.

3.4 TAI P3 results

In the TAI P3 analysis the same raw data provided by the geodetic GPS receivers are employed as in the GPS CP analysis discussed before, but the code measurements rather than the phase data are employed. Thereby the analysis is simplified, and in fact BIPM does the analysis on several links routinely as part of the monthly work of generating TAI. To fully assess the quality of the TAI P3 data it would have been necessary to resample the GPS CP measurements according to the epochs of the midpoints of the TAI P3 16-minute average values. This was postponed for a further refinement of this study. In Fig. 9, the frequency instability results obtained in the three links connecting to NPL are depicted. Only the link to OP connects two hydrogen masers and is suited to assess fully the merits of the TAI P3 analysis. The IEN (red) and PTB (blue) data are characterized by white frequency noise (slope −1/2) at averaging times around one day, and the observed instability is very close to the expectation value for a commercial caesium clock in the case of IEN and for the primary clock CS2 of PTB [16].

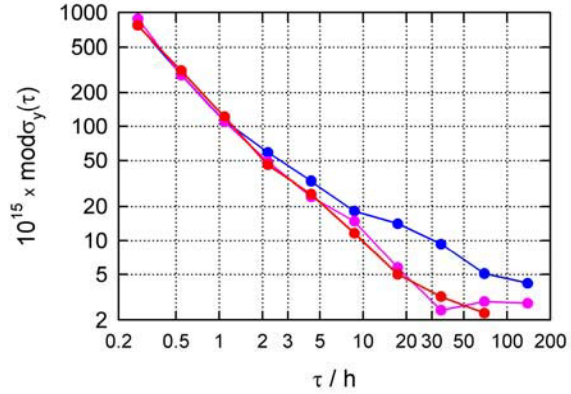

Fig 9 Relative frequency instability, expressed by $\mathrm{mod}\sigma_y(\tau)$, in the GPS TAI P3 comparison of UTC(NPL) with the maser at OP (magenta), and UTC(IEN) (red), and UTC(PTB) (blue).

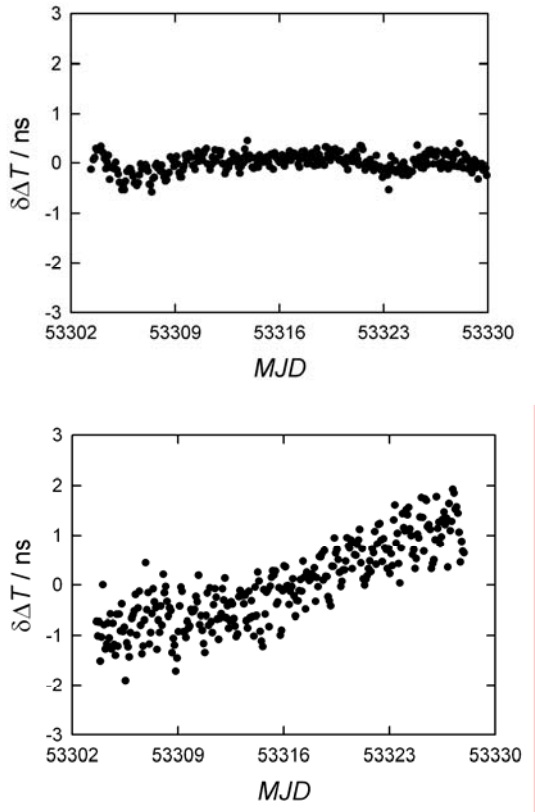

Fig. 10 Double differences of TWSTFT – GPS CP results, mean offset subtracted, upper: NPL – OP, lower: NIST – OP.

4. COMPARISONS

4.1 Discussion TW – GPS CP

During this campaign, the signal delays in the time transfer equipment were not of relevance since frequency comparisons, not true time comparisons, were the major concern. In this case only the variations of such signal delays matter since they could cause an erroneous frequency measurement result, which would in turn be detrimental for the success of the fountain comparisons [14]. TWSTFT data and GPS CP data obtained for the same epoch - within the 30 s separation of the GPS CP data - were compared. In Fig 10 two examples are depicted. In both cases, the mean offset in the data was subtracted. Whereas in the NPL-OP data all points are scattered almost within a 1-ns interval, a significant drift of about 2 ns is obvious in the NIST-OP data. If the latter was attributed to one of the techniques it would constitute a frequency error generated by the varying delays of only slightly less than one part in 10^{15} which is at the margin of being acceptable. A drift of the same magnitude is found when the link NPL-NIST is analyzed, but only half the magnitude is observed in case of NIST-PTB. No significant drift is visible in the links among NPL, OP, and PTB. When the stability of the data between OP and all four stations are analyzed, the results depicted in Fig. 11 are obtained. Since the data represent the combined uncertainty of two techniques, the PTB-NPL-OP data prove the capability of frequency comparisons with a measurement uncertainty of close to 1 part in 10^{15} at averaging times of 1 day, and the potential to do much better once a longer averaging time is accepted.

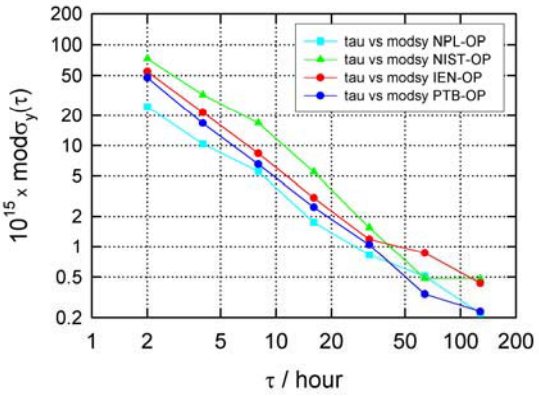

Fig. 11 Stability analysis of double differences TWSTFT – GPS CP for all links referenced to OP, see inset for the coding of the symbols.

4.2 Link comparisons and discussion of the frequency transfer uncertainty

In the graphs of Fig. 12 we compare the instability of a frequency comparison for the links NPL-OP, NPL-IEN, and IEN-OP using the three techniques. In all cases the same frequency references were used. In addition, the graphs contain the calculated instability for the double differences TWSTFT minus GPS CP. These graphs represent in a certain way the summary of the finding presented in different graphs before. We notice that the instability of GPS CP frequency transfer reaches the clocks' instability at about half a day; in the case of TWSTFT a full day is needed, and about 2 days are needed in the case of TAI P3. In case of longer averaging times there is no significant distinction between the three techniques visible from the graphs because of the clocks' instability. The instability of double differences reflects the long-term delay variations of the equipment involved. Since the equipment is the same for GPS CP and TAI P3 we cannot expect a difference in the long-term characteristics of the two techniques. This could of course be proven from a long-term comparison of TAI P3 and TWSTFT links which are routinely evaluated independent of a specific campaign.

In conclusion we compare the mean frequency differences obtained for selected links using the different techniques. The mean values were calculated in a straightforward manner, (δT(end) – δT(start)) / measurement interval. We chose the triplets of stations IEN-NPL-OP and NPL-OP-PTB. TAI P3 data with reference to the PTB maser were calculated based on its average frequency with respect to UTC(PTB) during the full period. The results are compiled in

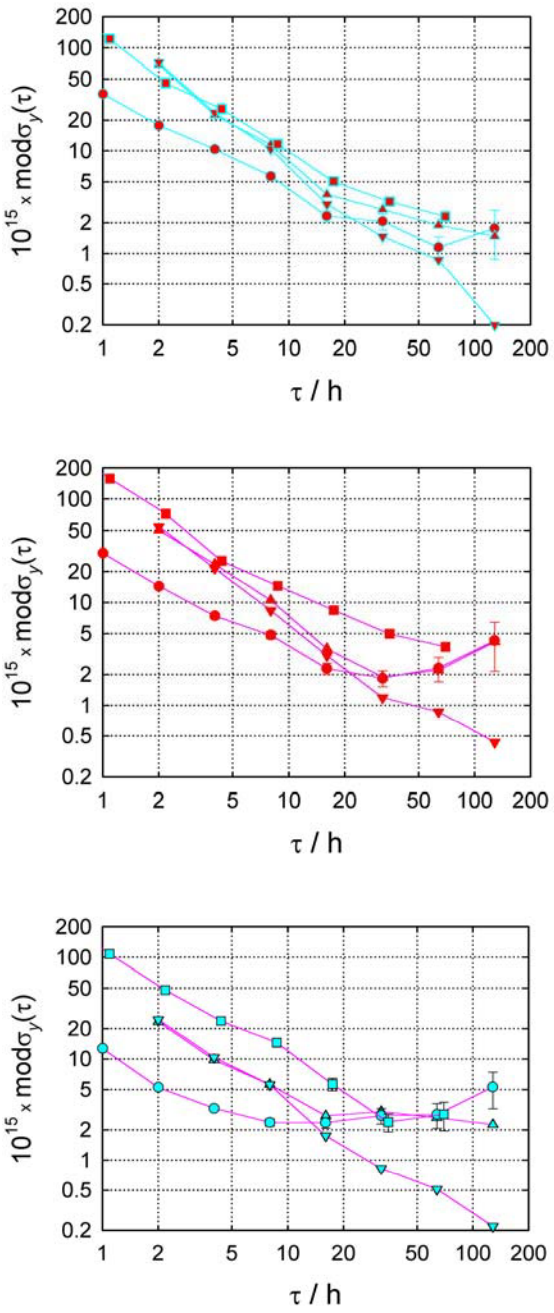

Fig. 12 Relative frequency instability, expressed by mod$\sigma_y(\tau)$, obtained for the three techniques, TAI P3 (squares), GPS CP (circles), and TWSTFT (symbol triangles up). In addition, the instability of double-differences TWSTFT – GPS CP (triangles down) has been illustrated for each link; upper graph: link IEN-NPL: middle graph: link IEN-OP; lower graph: link NPL-OP.

Tab. 3 Mean relative frequency differences in parts in 10^{15} during the interval 53304 to 53323 (inclusive, 20 days) between hydrogen masers at IEN, NPL, and OP, calculated using the three frequency comparison techniques, and the closure results

	IEN – OP	IEN – NPL	NPL – OP	Closure
TWSTFT	-430.8	-95.3	-336.1	0.6
GPS CP	-430.8	-94.5	-336.3	
TAI P3	-431.6	-95.1	-336.5	0.0

Tab. 4 Mean relative frequency differences in parts in 10^{15} during the interval 53304 to 53324 (inclusive, 21 days) between hydrogen masers at NPL, OP, and PTB and the closure results.

	PTB – NPL	PTB – OP	NPL – OP	Closure
TWSTFT	-74.24	-410.25	-336.08	0.07
GPS CP	-73.88	-410.13	-336.25	
TAI P3	-73.67	-410.07	-336.5	0.1

Tables 3 and 4. As said before, in the GPS CP analysis all loops comparing stations give zero. The maximum deviation within one column is 1×10^{-15}, but is typically much smaller.

5 CONCLUSIONS

We have reported on the results of a campaign originally stimulated by the intention to compare caesium fountain frequency standards in five institutes. GPS CP based analysis was used for the first time in such a campaign comprising a network of institutes. The campaign has provided much data not all of which could be presented in detail here. The following results are very encouraging:

1. TWSTFT in an intensified schedule and GPS CP analysis have allowed a frequency comparison between remote standards with a statistical uncertainty of 1×10^{-15} at averaging times of one day.
2. All studied techniques seem to be equally suited for the comparison of fountains without contributing significantly to the combined uncertainty of such comparisons, provided that a few days of averaging are allowed.
3. Systematic errors in frequency comparisons using any of the techniques did not exceed 1×10^{-15} during the period under study.

Further studies should address the following subjects

1. the nature and magnitude of drifts in the comparison to NIST;
2. the cause of the excessive noise observed in some TWSTFT links;
3. the optimum use of TAI P3 data, in continuation of previous work done by Petit and Jiang [20].

The low measurement noise provided by GPS CP at averaging times of less than one day makes it the first choice for use in comparisons among remote optical frequency standards since it is currently very challenging to operate such devices for extended periods. In the existing network such a comparison could be organized between NIST, NPL, and PTB, whose standards would be almost immediately ready for such purposes, and the experiences provided by the current study could be helpful in organizing such a comparison.

ACKNOWLEDGEMENT

The Corresponding Author would like to express his gratitude to his co-authors for providing guidance and rapid support. This work would not have been possible without the help of several individuals in the participating stations who took care of the operation of equipment, data retrieval, and analysis: Jürgen Becker, Davide Calonico, John Davis, Philippe Merck, Diego Orgiazzi, Valerio Pettiti, Dirk Piester, Jean-Yves Richard, David Valat. Thanks to Peter Whibberley for guidance in preparing the manuscript. The transponder on the IS-903 was provided free of charge by Intelsat Corp.

REFERENCES

[1] S. Bize et al., Advances in atomic fountains, *C. R. Physique*, **5** (2004), pp. 829-843.
[2] S. R. Jefferts et al., Accuracy evaluation of NIST-F1, *Metrologia* **39** (2002), pp. 321-336.
[3] S. Weyers, A. Bauch, R. Schröder, Chr. Tamm, The Atomic Caesium Fountain CSF1 of PTB, in Proc. 6th Symposium on Frequency Standards and Metrology (St. Andrews, Scotland, Sept. 2001), pp. 64-7
[4] K. Szymaniec, W. Chalupczak, P. B. Whibberley, S. N. Lea, D. Henderson, Evaluation of the primary frequency standard NPL-CsF1, *Metrologia* **42** (2005), pp. 49-57.
[5] F. Levi, L. Lorini, D. Calonico, A. Godone, IEN-CsF1 accuracy evaluation and two-way frequency comparison, *IEEE Trans. Ultrason. Ferroelec., and Freq. Control* **51** (2004), pp. 1216 – 1224.
[6] J. Levine, Time and frequency distribution using satellites, *Rep. Progr. Phys.* **65** (2002), pp. 1119 – 1164.
[7] D. Kirchner, Two-way Satellite Time and Frequency Transfer (TWSTFT): Principle, implementation, and current performance, Review of Radio Sciences 1996-1999, Oxford University Press, 1999, pp. 27-44.
[8] P. Defraigne, G. Petit, Time transfer to TAI using geodetic receivers, *Metrologia* **40** (2003), pp. 184-188.
[9] T. Schildknecht, G. Beutler, W. Gurtner, M. Rothacher, Towards subnanosecond GPS time transfer using geodetic processing techniques, in Proc. 4th European Frequency and Time Forum (Neuchâtel, Switzerland, 1990), pp. 335-346.
[10] K. M. Larson, J. Levine, Carrier-phase time transfer, *IEEE Trans. Ultrason. Ferroelec., and Freq. Control* **46** (1999), pp. 1001-1012.
[11] T. Parker, P. Hetzel, S. Jefferts, S. Weyers, L. Nelson, A. Bauch, J. Levine, First comparison of remote cesium fountains, in Proc. 2001 IEEE Freq. Control Symp. (Seattle, Washington, 2001), pp. 63-68.
[12] J. Ray, K. Senior, IGS/BIPM pilot project: GPS carrier phase for time/frequency transfer and timescale formation, *Metrologia* **40** (2003), pp. 270-288.
[13] R. Dach, L. G. Bernier, G. Dudle, T. Schildknecht, U. Hugentobler, Geodetic frequency transfer – actual developments in the AIUB-METAS collaboration, 19th EFTF (Besançon, France, 2005), in these Proceedings.
[14] D. Calonico et al., Comparison between remote Cs fountain primary frequency standards, 19th EFTF (Besançon, France, 2005), in these Proceedings.
[15] T. Parker, Hydrogen maser ensemble performance and characterization of frequency standards, in Proc. of the Joint meeting of the European Frequency and Time Forum and the IEEE International Freq. Control Symp. (Besançon, France, 1999), pp. 173-176.
[16] A. Bauch, The PTB primary clocks CS1 and CS2, *Metrologia* (2005) in press.
[17] Recommendation ITU-R TF.1153-1 "The operational use of two-way satellite time and frequency transfer employing PN time codes", ITU, Radiocommunication Study Group, Geneva, last update 2003.
[18] U. Hugentobler, S. Schaer, P. Fridez, eds., The Bernese GPS Software 4.2., University of Berne: Astronomical Institute, February 2001.
[19] D. W. Allan, C. Thomas, Technical directives for standardization of GPS time receiver software, *Metrologia* **31** (1994), pp. 69-79.
[20] G. Petit, Z. Jiang, Stability of geodetic time links and their comparison to two-way time transfer, in Proceedings of the 36th PTTI (Washington DC, 2004), in press.